



Research paper

## Microfluidic 3D intestine tumor spheroid model for efficient *in vitro* investigation of nanoparticulate formulations

Linda Elberskirch, Thorsten Knoll, Rebecca Königsmark, Janis Renner, Nadine Wilhelm, Hagen von Briesen, Sylvia Wagner\*

Fraunhofer Institute for Biomedical Engineering IBMT, Department Bioprocessing & Bioanalytics, Joseph-von-Fraunhofer-Weg 1, 66280, Sulzbach, Germany



## ARTICLE INFO

## Keywords:

Muco-adhesion  
Muco-permeability  
Fluidic chip  
Intestine cancer  
Mucus model  
Cancer  
Advanced drug screening  
Tumor targeting

## ABSTRACT

For the treatment of intestinal tumors by oral administration of drugs, the mucus layer of the intestine represents a barrier, but also a target possibility for drug. The use of nanoparticulate drug delivery systems is an important tool to improve the transport and accumulation of the drug on the target side. Therefore, specific *in vitro* test systems to simulate the conditions of an intestine tumor are necessary for the screening and efficiency testing of potential new nanoparticulate drug delivery systems. Here, we introduce a microfluidic 3D intestine tumor spheroid model, which allows to test functionalized nanoparticles and their ability to adsorb onto and permeate over a mucus layer under dynamic conditions. More specifically, the model consists of a 3D tumor spheroid with a mucus layer and microvilli on the surface, which is placed into a microfluidic chip system. The system incorporates a fluid flow, which is an important factor in nanoparticle residence time and uptake. To test the microfluidic 3D intestine tumor spheroid model, two different nanoparticle systems surface-coated with Carbopol® or Pluronic® F127 were produced to test the adsorption and permeation over the mucus layer. The data showed obvious adsorptive and permeable properties of uncoated and surface-coated nanoparticles in the static and dynamic system. The 3D intestine tumor spheroid model has the potential to significantly advance the preclinical development of new drugs like nanoparticles.

### 1. Introduction

Oral drug delivery is the preferred route for drug administration, as this is a non-invasive route with good patient compliance and cost-effectiveness [1,2]. The effectiveness of an orally administered drug compound depends on the bioavailability, which is mainly determined by the solubility and permeability [3]. The development of nanoparticles for the delivery of therapeutic agents has introduced new opportunities for improvement in medical treatment [4,5]. Accordingly, they are widely used in pharmaceutical research. Recent efforts have focused on developing target side specific nanoparticles, formulated by modifying nanoparticle surfaces with polymers or antibodies [6,7]. The need for a focused characterization on the surface modification and desired properties of the nanoparticulate drug delivery system requires preclinical studies. Therefore, *in vitro* test systems play an important role for the screening of potential new nanoparticulate drug delivery systems and their effectiveness. The common assessment method is the use of cell lines or primary cells in a 2D cell culture model. The Caco-2

adenocarcinoma cell line was extensively used for drug transport studies as an *in vitro* model of the intestinal mucosa [8,9]. These models also enable high-throughput screening of drugs [10]. However, simple 2D monolayer cell cultures like Caco-2 cell models are limited to simulate the complex structure of an *in vivo* tumor. Therefore, 3D tumor spheroids are an common and indispensable cell model for cancer drug screening, because of their analogy to *in vivo* tumors [11,12]. They are growing as cellular aggregates, which leads to multicellular contacts and the establishment of physicochemical gradients of nutrients, oxygen and pH. These gradients are crucial for the development of the characteristic structure of a tumor spheroids consisting of a vital outer cell layer, an intermediate layer of quiescent cells, and a necrotic core [13–15]. Similar structures are also found *in vivo* due to inefficient vascularization caused by rapid growth of the tumor tissue [14,16]. Additionally, the gradients effect the distribution, accumulation and efficacy of drugs in tumor tissue because of the limited mass transport to the non-vascularized tumor regions *in vivo* and inner layer of the tumor spheroids *in vitro* [14]. Despite the many advantages resulting from the

\* Corresponding author.

E-mail address: [sylvia.wagner@ibmt.fraunhofer.de](mailto:sylvia.wagner@ibmt.fraunhofer.de) (S. Wagner).

<https://doi.org/10.1016/j.jddst.2021.102496>

Received 22 December 2020; Received in revised form 19 March 2021; Accepted 20 March 2021

Available online 26 March 2021

1773-2247/© 2021 The Author(s).

Published by Elsevier B.V. This is an open access article under the CC BY-NC-ND license

(<http://creativecommons.org/licenses/by-nc-nd/4.0/>).

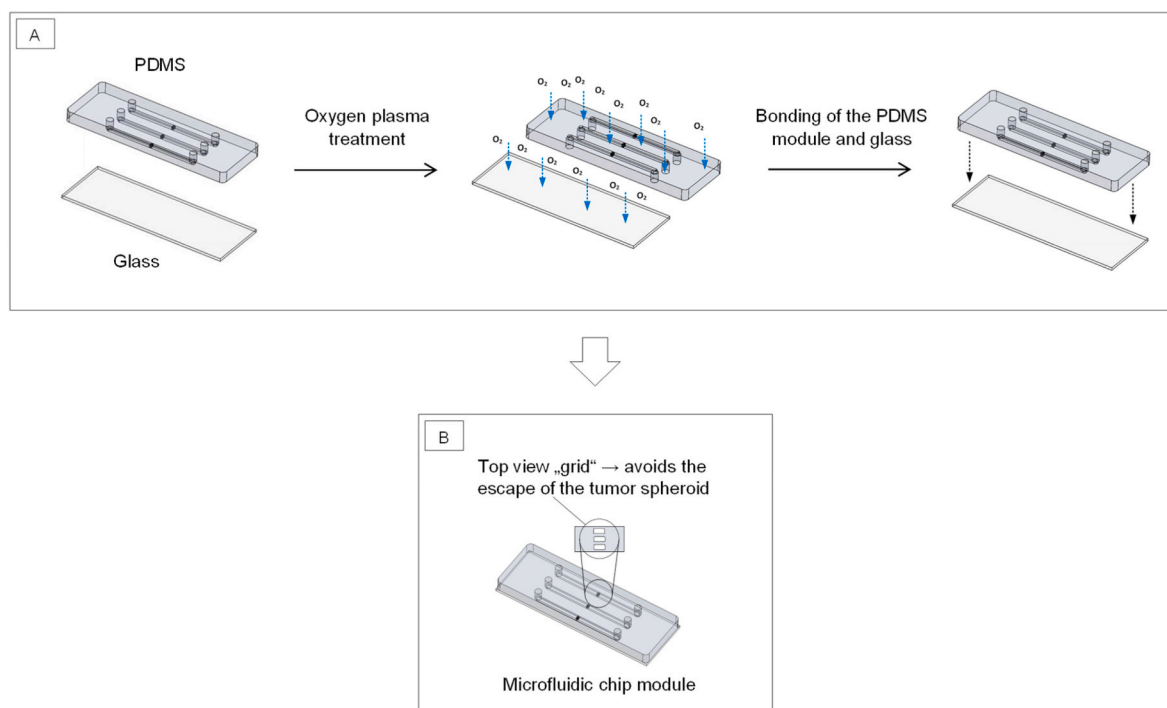


**Fig. 1.** Schematic drawing of the plasma bonding. (A) The PDMS form was bonded on a glass slide via  $O_2$  plasma activation to get a closed fluidic chip. (B) Top view of the microfluidic chip module with the “grid”, which avoids the escape of the tumor spheroids.

use of 3D tumor spheroids, the commonly used static conditions are not able to investigate the adhesion and permeation of a drug or nanoparticles [17]. To overcome these limitations, the use of microfluidic models in combination with cellular models offers an advanced test system for the drug development process [18,19]. For example, Toley et al. developed a microfluidic technique consisting of a static chamber with tumor spheroids of human colon adenocarcinoma cells (LS174T) and a connected microfluidic channel to simulate the blood vessels. Nanoparticulate formulations of doxorubicin were introduced into the microfluidic channel and their uptake and clearance were studied [20]. Another approach which used tumor spheroids in combination with a microfluidic platform was introduced by Mulholland et al. for drug screening. The used spheroids are biopsy-derived, and the microfluidic platform was generating a gradient of a chemotherapeutic drug to study dose-dependent efficacy [21]. The selected examples of microfluidic models in combination with tumor spheroids indicate the need for advanced *in vitro* test systems to study different aspects of the transport process of drugs and nanoparticulate formulations.

In this work, we focus on the possibility of nanoparticles to reach the target side by muco-adhesion and muco-permeation to a tumor of the gastrointestinal tract. The gastrointestinal tract has different barriers to be overcome by the nanoparticles before they reach the tumor. Furthermore, the adhesion and the uptake can be reduced because of the fluidic flow and peristaltic movements of the gastrointestinal tract [6]. One of the most important barriers is the mucus layer, which is hard to overcome for particle systems. To simulate this barrier, we developed a novel method to produce tumor spheroids with microvilli and a mucus layer on the surface based on the mucus-producing cell line HT29-MTX-E12. They were generated by a combination of static and dynamic culture conditions which resulted in a necrotic core, vital outer cell layer, microvilli, and a mucus layer on the surface. For the reflection of the dynamic environment inside the gastrointestinal tract, the 3D tumor spheroids were combined with a microfluidic chip system. The materials of the microfluidic module PDMS and glass in combination with a simple structure offer easy fabrication and high usability. In addition, the chip system can be cleaned and sterilized, resulting in a

re-useable and cost-effective chip system. By connecting a peristaltic pump, the dynamic intestinal environment could be simulated. Two strategies for the drug delivery and tumor targeting were used: muco-adhesion and muco-permeation. This was implemented by establishing two synthesis methods that allow nanoparticulate surface modification with the muco-adhesive compound Carbopol® or the muco-permeating compound Pluronic® F127.

We present the development of the advanced microfluidic 3D intestinal tumor spheroid model and the feasibility of using this preclinical test system to characterize the muco-adhering and muco-permeating properties of nanoparticles.

## 2. Materials and methods

### 2.1. Fabrication of the chip module/fluidic device design

The chip module was fabricated in the size of a microscopic slide (Fig. 1). It comprised a flow module with a microchannel having a width of 2 mm, a height of 1 mm and a length of 40 mm. Three micropillars with a height of 1 mm and a width of 0.6 mm were placed inside the microchannel in order to form a mechanical barrier for the spheroids. The microchannel with the micropillars and the fluid ports for inlet and outlet were fabricated by PDMS replication technique using Sylgard 184 (Dow Corning, Wiesbaden, Germany). Mould fabrication for the replication process was done by CNC milling of brass. Liquid PDMS was injected into the mould and after curing, the finished PDMS flow module was released from the mould. Assembly of the PDMS flow module with a glass slide was performed by plasma-assisted bonding of the two components using oxygen plasma activation [22]. The process was conducted at a power of 100 W, a pressure of 1 mbar and a plasma treatment time of 50 s (Diener electronic GmbH & Co KG, Ebhausen, Germany).

### 2.2. Tumor spheroid generation and characterization

#### 2.2.1. Generation

The human colon cancer cells HT29-MTX-E12 were obtained from

the European Collection of Cell Cultures (ECACC) and cultured in an incubator at 37 °C, 5% CO<sub>2</sub> and 95% relative air humidity. The used culture medium DMEM was supplemented with 2 mM glutamine, 1% non-essential amino acids (all purchased from Life Technologies GmbH, Darmstadt, Deutschland), antibiotics (1% Penicillin-Streptomycin, 10,000 UI/ml, Invitrogen GmbH) and 10% fetal bovine serum (Sigma-Aldrich GmbH, Steinheim, Germany). Cells were grown until 70–80% confluence. To generate spheroids, 4,500 cells per well were seeded in a corning spheroid microplate (Corning, Wiesbaden, Germany) and cultured over five days with medium change on every second day. On day five, the spheroids were transferred to a Cero cell culture tube and cultured under rotating conditions in a Cero (both purchased from OLS OMNI Life Science, Bremen, Germany). On day ten, batches of five spheroids were transferred to a 24-well cell suspension multiwell plate (Greiner Bio-One, Frickenhausen, Germany) and cultured under static conditions for two days until they built out a necrotic core similar to micrometastases *in vivo* [15]. The resulting tumor spheroids were used for the adsorption and permeation study within three days.

### 2.2.2. Histological analysis

The spheroids were washed for 5 min in PBS and fixed for 1 h in 10% formalin neutral buffered solution (Sigma-Aldrich, Steinheim, Germany). The tumor spheroids were incubated for 3 h in a sucrose (Sigma-Aldrich, Steinheim, Germany) gradient of 10%, 20% and 30% to cryoprotect them. Then they were embedded in Tissue Tek® embedding medium (Sakura Finetek USA, Inc., Torrance, United States of America) and stored at –80 °C until tissue sections were cut with a Leica cryostat CM3050 (Leica Biosystems GmbH, Nussloch, Germany). The slides were stained with nuclear red and alcian blue (Merck KGaA, Darmstadt, Germany) as declared by the manufacturer. Imaging was done by a bright field microscope.

### 2.2.3. Live-dead staining

The live-dead staining was performed at day twelve of the spheroid culture. Briefly, the spheroids were washed with PBS and then added to a 1 µmol/L calcein AM (green) and 1 µmol/L propidium iodide (red) (Sigma-Aldrich, Steinheim, Germany) solution. The samples were incubated for 10 min at 37 °C and then washed again with PBS. The images were taken with a fluorescence microscope CKX31 (Olympus, Hamburg, Germany). The overlay of the microscopic images was done with the software ImageJ 1.48v (Wayne Rasband, National Institute of Health, USA).

### 2.2.4. Scanning electron microscope images

To characterize the morphology and surface of the tumor spheroids, they were prepared for scanning electron microscopy in accordance to the protocol of Katsen et al. [23,24]. Therefore, the tumor spheroids were transferred to Transwell® cell culture inserts (Corning, Wiesbaden, Germany), washed in PBS and then fixed overnight in 2% glutaraldehyde in 0.1 M sodium cacodylate buffer. Then a post fixation followed by using a 2% osmium tetroxide solution in sodium cacodylate buffer. The samples were dehydrated by using an increasing series of ethanol solutions (10%, 20%, 30% ... up to 100%). The samples were coated with carbon and examined with a scanning electron microscope (EVO MA 10, Zeiss).

## 2.3. Synthesis and characterization of nanoparticles

The novel fluidic intestine-tumor-spheroid-model should be used to characterize nanoparticles regarding their ability to adsorb and permeate. Therefore, two kinds of nanoparticles with muco-adhesion and -permeating properties were produced by the modification of the nanoparticulate surface. Resomer RG 503H (Sigma-Aldrich, Steinheim, Germany) with a 50:50 lactide:glycolide ratio and a terminal carboxy group was chosen to obtain fast degrading PLGA nanoparticles [25]. In order to allow particle detection during the adhesion and permeation

studies, Lumogen® F Red 305 (LR) (provided by BASF AG, Ludwigshafen, Germany) was encapsulated. Muco-adhesive nanoparticles loaded with Lumogen® F Red 305 and a Carbopol® surface modification (NP1-LR-CP) were produced using the nanoprecipitation method (NP1) [26,27]. Carbopol® 971 P NF (Lubrizol, Hamburg, Germany) was used as modifying agent to provoke muco-adhesive function by polymer chain entanglement and hydrogen bridge bonding [28]. Therefore, 0.1% (w/v) Carbopol® 971 P NF was swollen overnight in distilled deionized water. For pretreatment procedure, the aqueous stock solution was neutralized by 2 M NaOH to pH 7. Viscosity was reduced by addition of 100 µl 10% HCl per 50 ml Carbopol® stock solution and finally adjusted to pH 7. For nanoparticle formation 20 mg Resomer RG 503H and 30 µg Lumogen® F Red 503 were dissolved in 1 ml DMSO as organic phase and added dropwise (0.5 ml min<sup>-1</sup>) to 20 ml of a 0.04% (w/v) Carbopol® aqueous phase under stirring (600 rpm). Organic solvent evaporation took place by further stirring for 5 h. Nanoparticles were collected by centrifugation at 21,000 g at 4 °C for 30 min and resuspended in PBS (pH 7.2). To generate the muco-permeating nanoparticles (NP2-LR-F127), Pluronic® F127 (Sigma-Aldrich, Steinheim, Germany) was used for the modification of the nanoparticle surface. The NP2-LR-F127 nanoparticles were synthesised by a double emulsion solvent evaporation method (NP2) [29]. 50 mg of PLGA and 100 µg Lumogen® F Red 503 were dissolved in an organic phase solution of 2 ml dichloromethane and 1 ml acetone. The organic phase was added dropwise to an aqueous phase (5 ml saponin 1% (v/w)) under sonication at 30% amplitude for 5 min in an ice-water bath. The emulsion was poured into another aqueous phase (20 ml saponin 1% (v/w)). The organic solvents were evaporated by stirring for 3 h (850 rpm). For further evaporation, the mixture was placed into a vacuum chamber for 30 min. The nanoparticles were then centrifuged at 21,000 g for 30 min and resuspended in an aqueous F127 solution (0.1% (v/w)). In addition, nanoparticles without surface modification were prepared with the synthesis methods NP1 and NP2 to study the influence of the muco-adhesive and muco-permeable properties of Carbopol® 971 P NF and Pluronic F127. Nanoparticles were stored at 4 °C until usage. The zeta potential and diameter of the nanoparticles were measured by dynamic light scattering, using Zetasizer Nano ZS (Malvern Instruments, Germany). 5 µl of nanoparticle suspension were diluted in 1 ml distilled deionized water. Nanoparticle concentration was determined by gravimetric analysis. 20 µl of a 1:2 diluted nanoparticle suspension was dried at 70 °C for at least 2 h in a drying cabinet (Binder GmbH, Tuttlingen, Germany) and equilibrated for 30 min in a vacuum chamber. The absolute mass of nanoparticle was determined in triplet using an ultra-micro scale (Mettler-Toledo AG, Gießen, Germany).

## 2.4. Adsorption and permeation studies

### 2.4.1. Static conditions

A batch of five spheroids was collected into a 24-well cell suspension plate. They were treated with the nanoparticles or the free Lumogen® F Red 305 compound diluted in culture medium with a concentration of 5 µM for 3 h inside the incubator. Additionally, an untreated and a solvent control were treated the same way.

### 2.4.2. Dynamic conditions

The studies were carried out inside an incubator at 37 °C, 5% CO<sub>2</sub> and 95% relative air humidity. The fluidic volume of 6 ml culture medium per chip module was pumped through the system by using a peristaltic pump with a speed of 100 µl/min. The resulting shear stress was calculated using the equation according to van Kooten et al.:  $\tau = 6\mu Q/(h^2w)$ , with the viscosity  $\mu$  in dyne s/cm<sup>2</sup>, the volumetric flow rate  $Q$  in cm<sup>3</sup>/s and  $h$  and  $w$  reflecting the width and height of the microfluidic channel [30]. The given channel dimensions (width 2 mm, height 1 mm), a flow rate of 100 µl/min and a viscosity of 10<sup>-3</sup> Pa s (for aqueous medium) result in a shear stress of 0.05 dyne/cm<sup>2</sup>. This value is within the range of other described *in vitro* systems [31,32]. To preheat

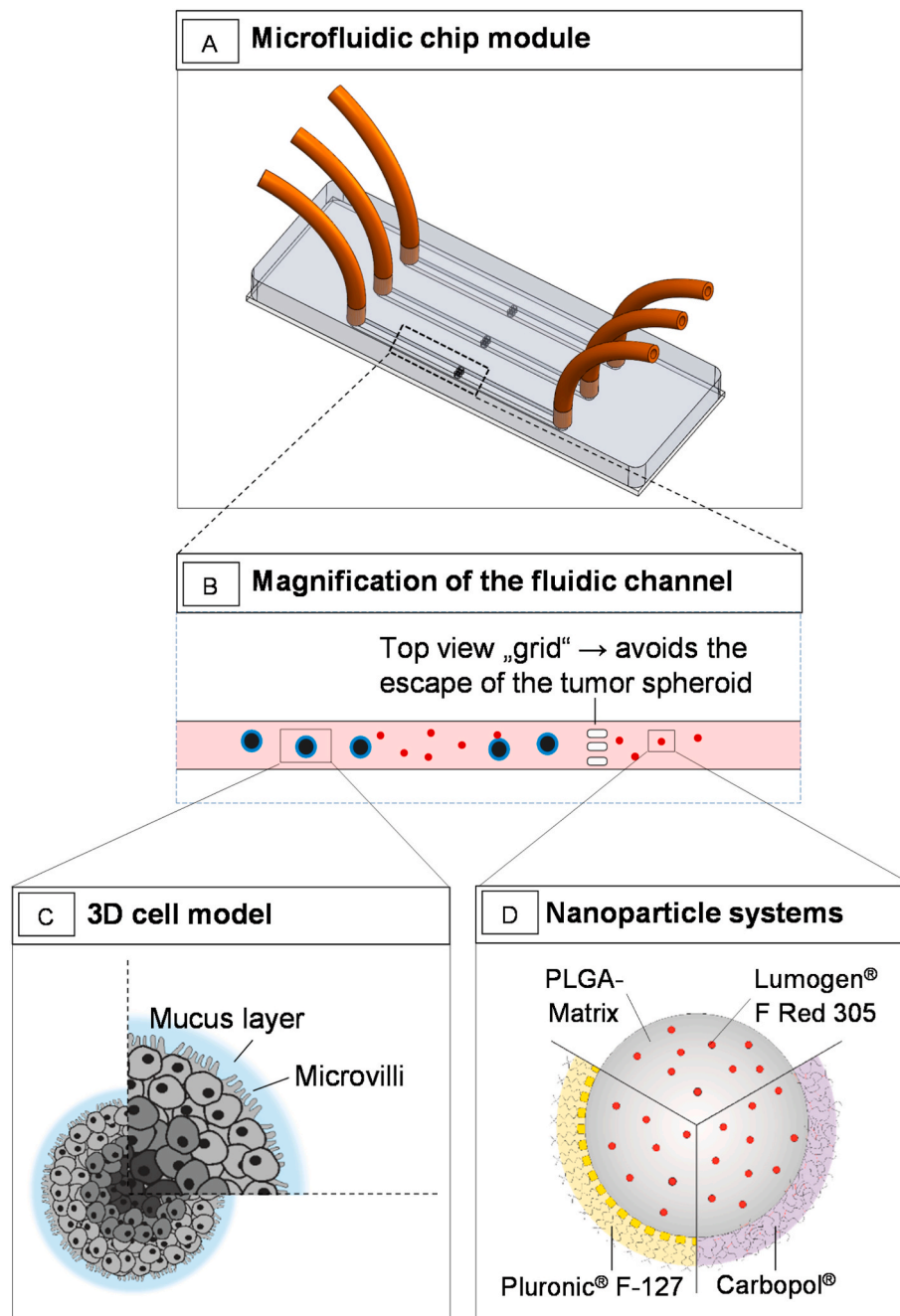


**Fig. 2.** Schematic drawing of the experimental set-up with the fluidic intestine tumor spheroid model. A) Microfluidic chip module and B) magnification of the fluidic channel. C) The 3D cell model consists of the cell line HT29-MTX-E12. They have microvilli and a mucus layer on the surface. D) Nanoparticle systems based on PLGA and with incorporated Lumogen® F Red 305 are additionally surface coated with Pluronic® F-127 or Carbopol®.

and equilibrate the system, it was integrated into the incubator and the pump was started 30 min before the experiments. Afterwards, the batch of five tumor spheroids was added into each fluidic channel of the chip module. The nanoparticles and the free Lumogen® red compound were admitted to the medium reservoir with a concentration of 5  $\mu\text{M}$ . The untreated and solvent cell control samples were also examined. After 3 h of incubation, the tumor spheroids were taken out from the channel and prepared for the further analysis.

#### 2.4.3. Analysis of the adsorbed and permeated compound

To qualify the adsorbed and permeated nanoparticles fluorescence imaging technique was used. The spheroids from the static and dynamic incubation were collected in a 96-well microplate. Bright field and

fluorescence pictures were taken with a microscope. For the quantification of the adsorbed and permeated nanoparticles, the amount of Lumogen® F Red 305 was measured via reversed-phase liquid chromatography. First the collected tumor spheroids were diluted in 200  $\mu\text{l}$  DMSO and lysed by using an ultrasound Sonicator® (BANDELIN electronic GmbH & Co. KG, Berlin, Germany) in pulse mode for 30 s and a frequency of 20 kHz. The samples were centrifuged at 300 g for 10 min. The supernatant was removed and measured by HPLC analysis using an Agilent infinity 1260 system (Agilent Technologies, Waldbronn, Germany). The system is equipped with an FLD detector and a Hypersil gold C18 column (4.6 mm  $\times$  150 mm, 5  $\mu\text{m}$ ). 100% acetonitrile were used as a mobile phase. The separation was carried out under isocratic conditions for 5 min with a flow rate of 1 ml/min and a

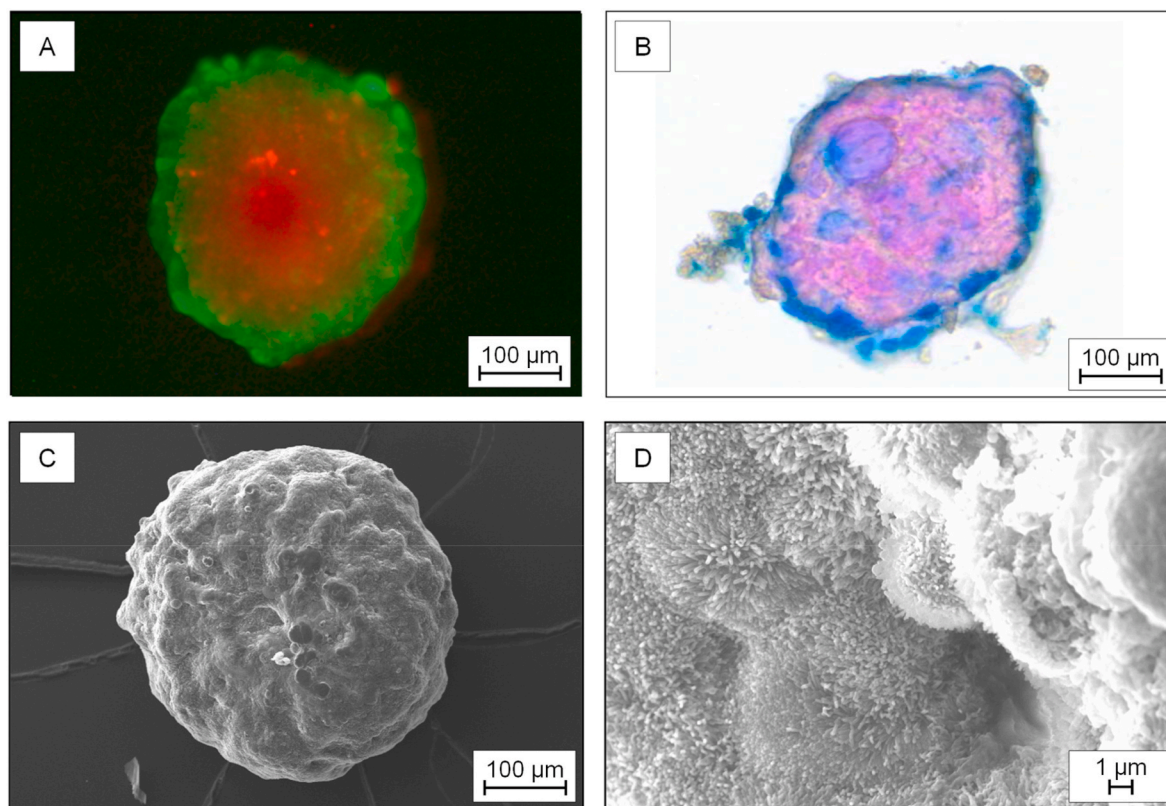


**Fig. 3.** Characterization of the 3D-tumor spheroids generated from the cell line HT29-MTX-E12.

A) Live-dead-staining: Simultaneous fluorescence staining of viable (calcein-AM, green) and dead cells (propidium iodid (PI), red). B) Histological stained spheroid: Nuclear fast red – cell nucleus; Alcian blue – acid mucosubstances and acetic mucins. C) Scanning electron microscopy of a spheroid and D) and scanning electron microscopy display of the microvilli on the surface.

temperature of 30 °C.

### 2.5. Cell viability assay

To investigate the cell viability of the tumor spheroids under static and dynamic conditions, an alamarBlue® assay (Thermo Fisher Scientific GmbH, Dreieich, Germany) was performed. A batch of five tumor spheroids was washed with PBS and the alamarBlue® reagent was added according to the manufacturer's instructions and incubated for 2 h. The fluorescence intensity was measured by using a TECAN infinite® 200 microplate reader (Tecan Group, Maennedorf, Switzerland) at an excitation wavelength of 560 nm and an emission wavelength of 610 nm.

### 2.6. Statistical analysis

The results were presented as mean  $\pm$  standard deviation. A comparison of the quantified free Lumogen® F Red 305 and incorporated into the nanoparticles was performed using the Welch *t*-test. P values less than <0.05 were considered as statistically significant.

## 3. Results and discussion

### 3.1. The microfluidic intestine-tumor-spheroid-model

Advances in the nanoparticle technology leads to the development of different nanocarriers. Specific preclinical models are needed to mimic the physiological conditions for evaluating the interactions between the nanoparticles with and without surface modification and the target cells. It is described that fluidic flow influences the ability of compounds and nanoparticles to adsorb and permeate to cells [33]. Enabling strong and selective binding to the target cells is important for their use in

nanomedicine. Static cell based assays have been developed to screen nanoparticles, in order to avoid large-scale and cost-intensive animal testing [34]. These tests could only observe certain aspects to the *in vivo* situation. To complete those standard methods, microfluidic devices can be used for supplementing the studies. We present an advanced microfluidic construction in combination with a cellular tumor model to test these conditions (Fig. 2). The cellular tumor model based on the mucus-secreting cell line HT29-MTX-E12. A mucus layer formed on the surface during the generation of the tumor spheroids due to the innovative generation method. The developed microfluidic intestinal tumor spheroid model enables the investigation of the efficacy of nanoparticles to adhere or permeate to a mucus layer. The materials used for the microfluidic module (silicone and glass) allow the use for the *in vitro* cultivation of cells. It is also possible to sterilize the microfluidic module by autoclaving and make it therefore reusable. In addition to the microfluidic module, the system requires also an external pump, tubing and connectors. The described test system is a helpful tool to study the interactions of the nanoparticles and the tumor spheroid under dynamic conditions. The handling of the new test system is more complex compared to conventional investigation methods where 2D cell cultivation is performed under static conditions. Nevertheless, the comparability of static *in vitro* test systems with *in vivo* studies is strongly limited. Thus, the use of dynamic model systems in the form of microfluidic models can be advantageous [35,36].

### 3.2. Characterization of the 3D cell model HT29-MTX-E12

Traditional 2D cell cultures like they are used in standard *in vitro* models are too simplified to simulate complex tumors inside the body. 3D cell cultures like spheroids can better reflect the *in vivo* situation. The cell line HT29-MTX-E12 was used as an intestine model to build 3D-

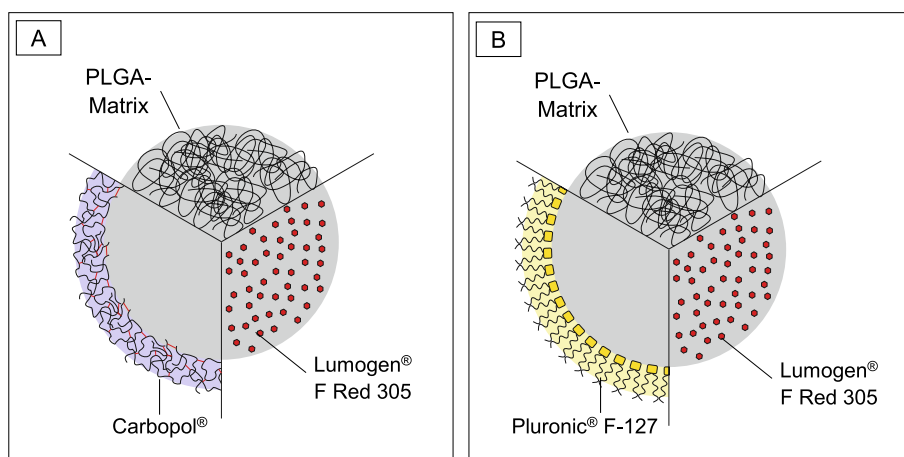


**Fig. 4.** Schematic drawing of the nanoparticle systems.

Two kinds of nanoparticle systems were developed based on a PLGA core. Lumogen® F Red 305 was incorporated for visualization and quantification of the nanoparticles. A) The nanoparticles with muco-adsorbing properties were synthesized with the nanoprecipitation method and coated with Carbopol®. B) Muco-permeable nanoparticles were synthesized with the double emulsion solvent evaporation method and modified with Pluronic® F-127.

**Table 1**

Physico-chemical characterization of the nanoparticles.

Measurement of the diameter, PDI, zeta potential and the Lumogen® F Red 305 (LR) concentration of the synthesised nanoparticles. NP1-LR: nanoparticles synthesised with nanoprecipitation and incorporated Lumogen® F Red 305; NP1-LR-CP: nanoparticles synthesised with nanoprecipitation, incorporated Lumogen® F Red 305 and surface modification with Carbopol®; NP2-LR: nanoparticles synthesised with double emulsion solvent evaporation and incorporated Lumogen® F Red 305; NP2-LR-F127: nanoparticles synthesised with double emulsion solvent evaporation, incorporated Lumogen® F Red 305 and modification with Pluronic® F-127.

Nanoparticle	Parameter			
	Hydrodynamic diameter [nm]	PDI	Zeta potential [mV]	LR-concentration [ $\mu\text{g/mL}$ ]
NP1-LR	$118.2 \pm 2.3$	$0.07 \pm 0.02$	$-33.2 \pm 1.2$	$61.1 \pm 5.3$
NP1-LR-CP	$132.2 \pm 1.8$	$0.08 \pm 0.01$	$-43.5 \pm 0.8$	$38.2 \pm 4.6$
NP2-LR	$114.2 \pm 2.1$	$0.06 \pm 0.02$	$-34.2 \pm 1.6$	$605.2 \pm 9.8$
NP2-LR-F127	$119.1 \pm 1.8$	$0.08 \pm 0.01$	$-42.5 \pm 1.5$	$563.1 \pm 10.2$

tumor spheroids. They consist of a vital outer cell layer and a necrotic core (Fig. 3, A), which displays physicochemical gradients similar to micro-metastases. The used HT29-MTX-E12 cells are goblet cells, which are able to produce mucus (Fig. 3, B). They are also able to build microvilli on the surface (Fig. 3, D).

The results of preclinical *in vitro* cell culture tests form the basis for *in vivo* studies. However, standard static cell culture models do not sufficiently simulate *in vivo* conditions. For example, in standard static test systems, the cell model is constantly exposed to the test compound, which does not correspond to the physiological conditions. This limits the significance of *in vitro* data for translation of drug dosages to *in vivo* studies [37,38]. A further limitation of those standard static test systems is the use of 2D-cell culture models with cells growing in flat layers on plastic surfaces, which could not mimic the *in vivo* state [39]. Microfluidic 3D cell models have the potential to overcome some of the limitations of conventional 2D-cell culture models [12]. Our developed 3D tumor spheroid shows the typical physicochemical gradients because of the vital outer cell layer and a necrotic core. The microvilli and a mucus layer on the surface are additional feature of our development. These properties make our 3D tumor spheroid a good model to simulate an intestine tumor.

### 3.3. Basic characterization of the nanoparticles

The nanoparticles were synthesised by two different methods: nanoprecipitation and double emulsion solvent evaporation (Fig. 4). Poly(lactid-co-glycolid) (PLGA) was used as a basic material. It is biodegradable and approved by the United States Food and Drug Administration (U.S. FDA) and the European Medicine Agency (EMA) [40]. To visualize and quantify the nanoparticles the fluorescence dye Lumogen® F Red 305 was incorporated.

The nanoparticles synthesised with the nanoprecipitation method with surface modification had a mean size of  $132.2 \pm 1.8$  nm and a PDI

of  $0.08 \pm 0.01$ . The zeta potential measurement had a mean of  $-43.5 \pm 0.8$  mV. The quantification of the incorporated Lumogen® F Red 305 quantity obtained  $38.2 \pm 4.6$   $\mu\text{g/mL}$ . Control nanoparticles synthesised with the nanoprecipitation method without surface modification had a mean size of  $118.2 \pm 2.3$  nm and a PDI of  $0.07 \pm 0.02$ . The zeta potential measurement had a mean of  $-33.2 \pm 1.2$  mV and an incorporated Lumogen® F Red 305 quantity of  $61.1 \pm 5.3$   $\mu\text{g/mL}$ . The nanoparticles prepared with the double emulsion solvent evaporation with Lumogen® F Red 305 had a mean size of  $119.1 \pm 1.8$  nm. A poly dispersity index (PDI) of  $0.08 \pm 0.01$  indicates a homogeneous particle distribution and zeta potential was  $-42.5 \pm 1.5$  mV. The amount of the incorporated fluorescence dye quantified via HPLC had a mean of  $563.1 \pm 10.2$   $\mu\text{g/mL}$  nanoparticle solution. The analogue produced nanoparticles without a Pluronic® F127 surface modification had a mean size of  $114.2 \pm 2.1$  nm and a PDI of  $0.06 \pm 0.02$ . The zeta potential measurement had a mean of  $-34.2 \pm 1.6$  mV and an incorporated Lumogen® F Red 305 quantity of  $605.2 \pm 9.8$   $\mu\text{g/mL}$  (see also Table 1). The used synthesis methods nanoprecipitation and double emulsion solvent evaporation resulted in different nanoparticle characteristics. The main differences were found in the amount of the incorporated Lumogen® F Red 305 quantity. This was about 10–15 times higher with the emulsion solvent evaporation method compared to the nanoprecipitation method. Additionally, the incorporated Lumogen® F Red 305 quantity decreases to 23  $\mu\text{g/mL}$  after the modification with Carbopol®. This could be an indication that the Lumogen® F Red 305 partially adhered to the surface of the nanoparticle and detached during the modification process.

A viability assay was performed to evaluate the influence of dynamic flow on tumor spheroids. The fluid was transported through the fluidic chip module in peristaltic movements, simulating the intestinal movement. This makes it possible to investigate the dynamic barrier properties caused by peristaltic movements in the intestine due to a horizontal flow over the mucus layer [41]. The steric barrier properties of the mucus layer strongly limit the adhesion and permeation of

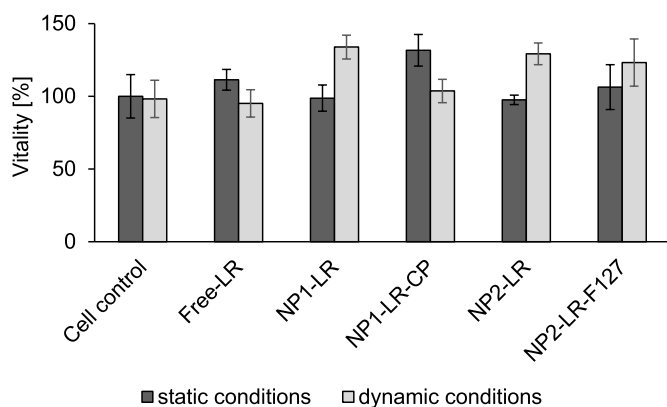


**Fig. 5.** Viability assay of HT29-MTX-E12 tumor spheroids after static and dynamic incubation of the nanoparticles.

Effect of dynamic conditions on cell viability of the HT29-MTX-E12 tumor spheroids after 3 h of testing in comparison to the static conditions. Cell viability and growth were assessed by the alamarBlue® assay and normalized to values on the cell control. Values represent averages  $\pm$  SD ( $n = 3$ ). NP1-LR: nanoparticles synthesised with nanoprecipitation and incorporated Lumogen® F Red 305; NP1-LR-CP: nanoparticles synthesised with nanoprecipitation, incorporated Lumogen® F Red 305 and surface modification with Carbopol®; NP2-LR: nanoparticles synthesised with double emulsion solvent evaporation and incorporated Lumogen® F Red 305; NP2-LR-F127: nanoparticles synthesised with double emulsion solvent evaporation, incorporated Lumogen® F Red 305 and modification with Pluronic® F-127. Static conditions: test performed in suspension well plate, dynamic conditions: test performed in the microfluidic chip module.

nanoparticulate systems [42]. Therefore, it represents an important point in the investigation of muco-adhesive and muco-permeable nanoparticles. The dynamic condition in microfluidic test systems triggers fluidic shear stress, which can have an influence on the cell viability [43]. For example, a study of HL60 cells (leukemia cell line) investigated the effects of shear stress on cell viability. This was reduced by  $> 11.8\%$  when cells were cultivated under fluidic flow compared to cells cultivated under static conditions [26]. In the present study, the viability assay showed no significant difference between static and dynamic conditions (Fig. 5), ruling out that there is no effect within the 3 h of testing.

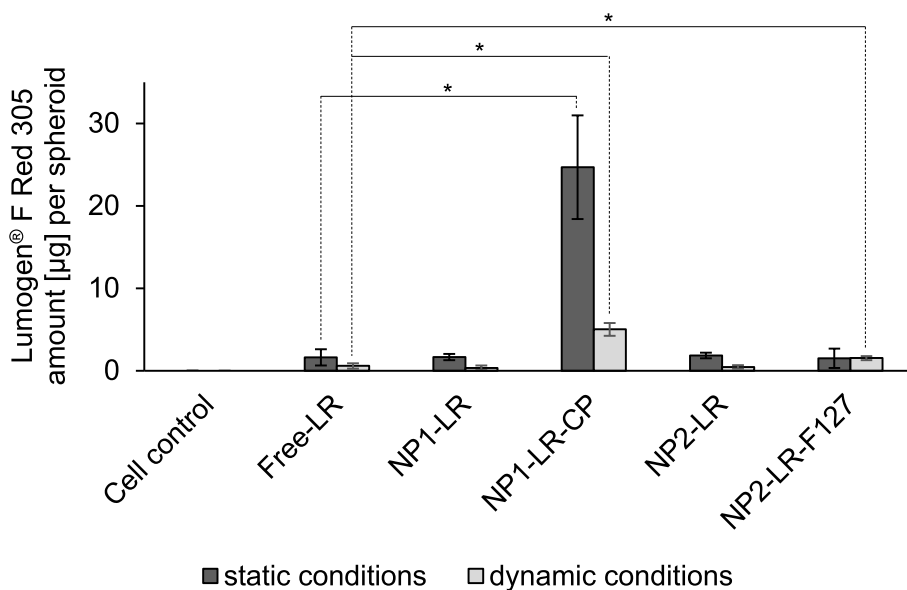


**Fig. 6.** HPLC quantification of Lumogen® F Red 305. The amount of Lumogen® F Red 305 was calculated per spheroid in  $\mu\text{g}$  ( $n = 4$ ,  $k = 5$ ). \*Significant deviation according to the Welch  $t$ -test with a significance level of a  $P$  value of  $< 0.05$  is considered statistically significant comparison of the free and incorporated Lumogen® F Red 305 grouped into static and dynamic conditions. NP1-LR: nanoparticles synthesised with nanoprecipitation and incorporated Lumogen® F Red 305; NP1-LR-CP: nanoparticles synthesised with nanoprecipitation, incorporated Lumogen® F Red 305 and surface modification with Carbopol®; NP2-LR: nanoparticles synthesised with double emulsion solvent evaporation and incorporated Lumogen® F Red 305; NP2-LR-F127: nanoparticles synthesised with double emulsion solvent evaporation, incorporated Lumogen® F Red 305 and modification with Pluronic® F-127. Static conditions: test performed in suspension well plate, dynamic conditions: test performed in the microfluidic chip module.

### 3.4. Evaluation of adsorption and permeation properties of the nanoparticles

To study the adsorption and permeation of nanoparticles to the tumor spheroids under static and dynamic conditions, the nanoparticles were added into the test system and incubated over 3 h. After the incubation, spheroids were lysed and the Lumogen® F Red 305 content was analysed by high performance liquid chromatography (HPLC). We observed the muco-adsorbed or muco-permeated Lumogen® F Red 305 quantity, which was added as free compound or incorporated into nanoparticles. The analysed amount of the free LR and Lumogen® F Red 305 incorporated into NP1-LR, NP2-LR and NP2-LR-F127 was comparable. The measured Lumogen® F Red 305 quantity was significant higher after incorporation into the nanoparticulate formulation NP2-LR-F127 under dynamic conditions and NP1-LR-CP under static and dynamic conditions compared to the incubated free LR (Fig. 6). Overall, the HPLC measurements showed that the compound Lumogen® F Red 305 can adsorb to the HT29-MTX-E12 tumor spheroids as free compound and incorporated into nanoparticles. Additionally, the free LR and the nanoparticles loaded with Lumogen® F Red 305 could be displayed on the surface of the tumor spheroids with fluorescence microscopy (Fig. 7). The tumor spheroids have a mean size of  $566 \pm 46 \mu\text{m}$ . The images show a fluorescence signal on the surface of the tumor spheroid of the NP1-LR-CP and NP2-LR-F127.

The use of muco-adhesive or muco-permeable compounds can influence the targeted transport of drugs to the mucus layer. For the examination of the ability of nanoparticulate muco-adsorption or muco-permeation, the 3D intestine tumor spheroid with the mucus layer and microvilli on the surface was developed. One example of a highly muco-adhesive synthetic polymer is polyacrylic acid (PAA). The muco-adhesive properties base on the ability of PAA carboxyl groups to form strong hydrogen bonds with the oligosaccharide chains of the mucins. In addition, the polymers and the mucin fibers are physically entangled [44]. One group of PAA polymers are carbopoles, which are frequently used in the pharmaceutical industry as emulsifiers and gelling agents for topical formulations [45]. They also exhibit strong muco-adhesive properties due to mechanical interpenetration of the polymer chains, the formation of hydrogen bonds and ionic interactions [46]. To achieve muco-permeation, the poloxamer Pluronic® F-127 can be used for surface modification of nanoparticles. Due to its hydrophilic and hydrophobic polymer chains, it has amphiphilic properties. Therefore, the modification of nanoparticles with Pluronic® F127 leads to a

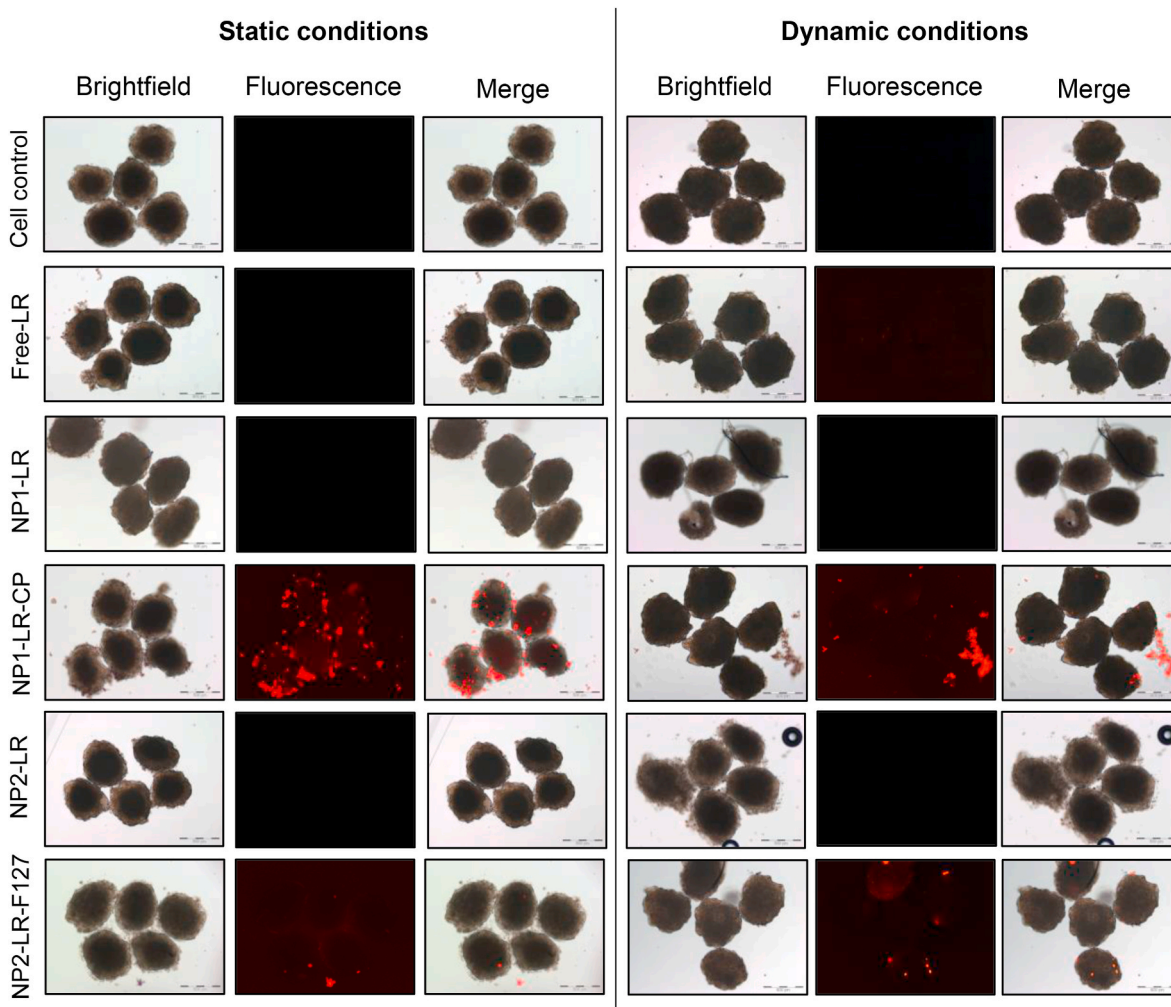


**Fig. 7.** Microscope images of HT29-MTX-E12 tumor spheroids after static and dynamic incubation of the nanoparticles for 3 h. Microscopic observation of HT29-MTX-E12 tumor spheroids and the adhered or permeated nanoparticles loaded with Lumogen® F Red 305. NP1-LR: nanoparticles synthesised with nanoprecipitation and incorporated Lumogen® F Red 305; NP1-LR-CP: nanoparticles synthesised with nanoprecipitation, incorporated Lumogen® F Red 305 and surface modification with Carbopol®; NP2-LR: nanoparticles synthesised with double emulsion solvent evaporation and incorporated Lumogen® F Red 305; NP2-LR-F127: nanoparticles synthesised with double emulsion solvent evaporation, incorporated Lumogen® F Red 305 and modification with Pluronic® F-127. Static conditions: test performed in suspension well plate, dynamic conditions: test performed in the microfluidic chip module.

reduction of interactions between the nanoparticulate drug carrier system and the mucus layer. In addition, this modification leads to a high nanoparticle stability [47]. The results showed that the adhesion of Carbopol® modified nanoparticles was significantly higher compared to non-modified control nanoparticles and nanoparticles modified with Pluronic® F-127. This confirms that surface modification of the nanoparticles with Carbopol® leads to improved muco-adhesion. Additionally, the fluidic flow influences the amount of the adsorbed or permeated compound, which reduces the residence time and uptake. This resulted in an overall lower amount of Lumogen® F Red 305 in the dynamic system compared to the static incubation, due to the longer contact time in the static environment and absence of shear forces occurring in flow, which could minimize particle attachment. A reduction of the uptake of nanoparticles in dynamic systems compared to static system is often described in the literature. This confirmed the poor transferability of static *in vitro* test results to *in vivo* studies and clarify the important role of dynamic test systems in preclinical research [48]. The reasons for the reduced uptake are shear stress, reduced exposure time of the individual nanoparticles to the cell surface and the formation of aggregates under fluidic conditions which could not be simulated in static *in vitro* test systems [49,50]. The developed intestinal tumor model provides a helpful tool to simulate these conditions. In addition, the developed 3D

tumor spheroid helps to study the expected functionality of nanoparticles like muco-adhesion or muco-permeation, because of its microvilli and mucus layer on the surface. Specifically, the current study highlights how an advanced microfluidic test system combined with a 3D cell model complements standard static cell assays, thus enabling a more comprehensive assessment of the targeting ability of nanoparticles. Therefore, the test system introduced here enables a selection of promising nanoparticulate formulations for the transport of a compound to an intestinal tumor.

#### 4. Conclusion

We demonstrated a new intestine tumor spheroid model combined with a microfluidic chip modul that can be used as a new *in vitro* tool to test the ability of nanoparticles to adsorb and permeate to a cancer model. A special feature of the 3D tumor spheroid are the microvilli and mucus layer on the surface, which could simulate the surface properties of an *in vivo* intestine tumor. Thus, the system provides a specific testing method, which could bridge the gap between standard *in vitro* test systems and *in vivo*. Complementary, we engineered nanoparticles, which can adsorb and permeate to mucus. The tested nanoparticles with a Carbopol® modification showed an increasing adsorption to the tumor

spheroids compared to the free test compound Lumogen® F Red 305 under static and dynamic conditions. This was analysed by HPLC and microscopic observation.

In summary, the nanoparticle-cell interactions can be studied under fluidic flow in this new microfluidic 3D intestine tumor spheroid model. With this approach, it is possible to achieve more accurate information and optimization of nanoparticles used as drug delivery systems. This results in an improved transferability of *in vitro* studies to *in vivo* studies and also contributes to a reduction of animal experiments within the meaning of 3Rs concept (Replacement, Reduction, Refinement) [51].

#### CRedit authorship contribution statement

**Linda Elberskirch:** Methodology, Validation, Formal analysis, Investigation, Writing – original draft, Writing – review & editing. **Thorsten Knoll:** Methodology, Writing – original draft, Writing – review & editing. **Rebecca Königsmark:** Validation, Investigation. **Janis Renner:** Validation, Investigation. **Nadine Wilhelm:** Methodology, Writing – review & editing, Supervision. **Hagen von Briesen:** Conceptualization, Methodology, Writing – review & editing, Supervision, Project administration, Funding acquisition. **Sylvia Wagner:** Conceptualization, Methodology, Writing – review & editing, Supervision, Project administration, Funding acquisition.

#### Declaration of competing interest

The authors declare that they have no known competing financial interests or personal relationships that could have appeared to influence the work reported in this paper.

#### Acknowledgements

This work was financially supported by the BMBF (13N13424).

#### References

- [1] B. Homayun, X. Lin, H.J. Choi, Challenges and recent progress in oral drug delivery systems for biopharmaceuticals, *Pharmaceutics* 11 (2019), <https://doi.org/10.3390/pharmaceutics11030129>.
- [2] P. Viswanathan, Y. Muralidaran, G. Ragavan, Challenges in oral drug delivery: a nano-based strategy to overcome, *Nanostructures Oral Med* (2017) 173–201, <https://doi.org/10.1016/B978-0-323-47720-8.00008-0>.
- [3] G.L. Amidon, H. Lennernäs, V.P. Shah, J.R. Crison, A theoretical basis for a biopharmaceutical drug classification: the correlation of *in vitro* drug product dissolution and *in vivo* bioavailability, *Pharm. Res. An Off. J. Am. Assoc. Pharm. Sci.* 12 (1995) 413–420, <https://doi.org/10.1023/A:1016212804288>.
- [4] M.A. Shetab Boushehri, A. Lamprecht, Nanoparticles as drug carriers: current issues with *in vitro* testing, *Nanomedicine* 10 (2015) 3213–3230, <https://doi.org/10.2217/nmm.15.154>.
- [5] A.Z. Wang, F. Gu, L. Zhang, J.M. Chan, A. Radovic-Moreno, M.R. Shaikh, O. C. Farokhzad, Biofunctionalized targeted nanoparticles for therapeutic applications, *Exp. Opin. Biol. Ther.* 8 (2008) 1063–1070, <https://doi.org/10.1517/14712598.8.8.1063>.
- [6] B. Haley, E. Frenkel, Nanoparticles for drug delivery in cancer treatment, *Urol. Oncol. Semin. Orig. Investig.* 26 (2008) 57–64, <https://doi.org/10.1016/j.urolonc.2007.03.015>.
- [7] E. Russo, F. Selmin, S. Baldassari, C.G.M. Gennari, G. Caviglioli, F. Cilirzo, P. Minghetti, B. Parodi, A Focus on Mucoadhesive Polymers and Their Application in Buccal Dosage Forms, 2016, <https://doi.org/10.1016/j.jddst.2015.06.016>.
- [8] I. Hubatsch, E.G.E. Ragnarsson, P. Artursson, Determination of drug permeability and prediction of drug absorption in Caco-2 monolayers, *Nat. Protoc.* 2 (2007) 2111–2119, <https://doi.org/10.1038/nprot.2007.303>.
- [9] A.A. Date, J. Hanes, L.M. Ensign, Nanoparticles for oral delivery: design, evaluation and state-of-the-art, *J. Contr. Release* 240 (2016) 504–526, <https://doi.org/10.1016/j.jconrel.2016.06.016>.
- [10] M. Dhandapani, A. Goldman, Preclinical cancer models and biomarkers for drug development: new Technologies and emerging tools, *J. Mol. Biomarkers Diagn.* (2017), <https://doi.org/10.4172/2155-9929.1000356>, 08.
- [11] J. Friedrich, C. Seidel, R. Ebner, L.A. Kunz-Schughart, Spheroid-based drug screen: considerations and practical approach, *Nat. Protoc.* 4 (2009) 309–324, <https://doi.org/10.1038/nprot.2008.226>.
- [12] K.E. Sung, D.J. Beebe, Microfluidic 3D models of cancer, *Adv. Drug Deliv. Rev.* 79–80 (2014) 68–78, <https://doi.org/10.1016/j.addr.2014.07.002>.
- [13] K. Groebe, W. Mueller-Klieser, Distributions of oxygen, nutrient, and metabolic waste concentrations in multicellular spheroids and their dependence on spheroid parameters, *Eur. Biophys. J.* 19 (1991) 169–181, <https://doi.org/10.1007/BF00196343>.
- [14] G. Mehta, A.Y. Hsiao, M. Ingram, G.D. Luker, S. Takayama, Opportunities and challenges for use of tumor spheroids as models to test drug delivery and efficacy, *J. Contr. Release* 164 (2012) 192–204, <https://doi.org/10.1016/j.jconrel.2012.04.045>.
- [15] S. Nath, G.R. Devi, Three-dimensional culture systems in cancer research: focus on tumor spheroid model, *Pharmacol. Ther.* 163 (2016) 94–108, <https://doi.org/10.1016/j.pharmthera.2016.03.013>.
- [16] S.C. Brüningk, I. Rivens, C. Box, U. Oelfke, G. ter Haar, 3D tumour spheroids for the prediction of the effects of radiation and hyperthermia treatments, *Sci. Rep.* 10 (2020) 1, <https://doi.org/10.1038/s41598-020-58569-4>.
- [17] A. Ozcelikkale, H.R. Moon, M. Linnes, B. Han, *In vitro* microfluidic models of tumor microenvironment to screen transport of drugs and nanoparticles, *Wiley Interdiscip. Rev. Nanomedicine Nanobiotechnology.* 9 (2017), <https://doi.org/10.1002/wnan.1460>.
- [18] S. Damiati, U.B. Kompella, S.A. Damiati, R. Kodzius, Microfluidic devices for drug delivery systems and drug screening, *Genes* 9 (2018), <https://doi.org/10.3390/genes9020103>.
- [19] P. Cui, S. Wang, Application of microfluidic chip technology in pharmaceutical analysis: a review, *J. Pharm. Anal.* 9 (2019) 238–247, <https://doi.org/10.1016/j.jpfa.2018.12.001>.
- [20] B.J. Toley, Z.G. Tropeano Lovatt, J.L. Harrington, N.S. Forbes, Microfluidic technique to measure intratumoral transport and calculate drug efficacy shows that binding is essential for doxorubicin and release hampers Doxil, *Integr. Biol.* 5 (2013) 1184, <https://doi.org/10.1039/c3ib40021b>.
- [21] T. Mulholland, M. McAllister, S. Patek, D. Flint, M. Underwood, A. Sim, J. Edwards, M. Zagnoni, Drug screening of biopsy-derived spheroids using a self-generated microfluidic concentration gradient, *Sci. Rep.* 8 (2018) 14672, <https://doi.org/10.1038/s41598-018-33055-0>.
- [22] C.W. Beh, W. Zhou, T.H. Wang, PDMS-glass bonding using grafted polymeric adhesive—alternative process flow for compatibility with patterned biological molecules, *Lab Chip* 12 (2012) 4120–4127, <https://doi.org/10.1039/c2lc40315c>.
- [23] A.D. Katsen, B. Vollmar, P. Mestres-Ventura, M.D. Menger, Cell surface and nuclear changes during TNF- $\alpha$ -induced apoptosis in WEHI 164 murine fibrosarcoma cells. A correlative light, scanning, and transmission electron microscopic study, *Virchows Arch.* 433 (1998) 75–83, <https://doi.org/10.1007/s004280050219>.
- [24] A. Katsen-Globa, N. Puetz, M.M. Gepp, J.C. Neubauer, H. Zimmermann, Study of SEM preparation artefacts with correlative microscopy: cell shrinkage of adherent cells by HMDS-drying, *Scanning* 38 (2016) 625–633, <https://doi.org/10.1002/sca.21310>.
- [25] R.A. Jain, The manufacturing techniques of various drug loaded biodegradable poly(lactide-co-glycolide) (PLGA) devices, <https://eurekamag.com/pdf/011/011524128.pdf>, 2000. (Accessed 16 November 2018).
- [26] M. Rojnik, P. Kocbek, F. Moret, C. Compagnin, L. Celotti, M.J. Bovis, J. H. Woodhams, A.J. MacRobert, D. Scheglmann, W. Helfrich, M.J. Verkaik, E. Papini, E. Reddi, J. Kos, *In vitro* and *in vivo* characterization of temporofin-laden PEGylated PLGA nanoparticles for use in photodynamic therapy, *Nanomedicine* 7 (2012) 663–677, <https://doi.org/10.2217/nmm.11.130>.
- [27] X. Niu, W. Zou, C. Liu, N. Zhang, C. Fu, Modified nanoprecipitation method to fabricate DNA-loaded PLGA nanoparticles modified nanoprecipitation method, *Drug Dev. Ind. Pharm.* 35 (2009) 1375–1383, <https://doi.org/10.3109/03639040902939221>.
- [28] A. Sosnik, J. das Neves, B. Sarmento, Mucoadhesive polymers in the design of nano-drug delivery systems for administration by non-parenteral routes: a review, *Prog. Polym. Sci.* 39 (2014) 2030–2075, <https://doi.org/10.1016/J.PROGPOLYMSCI.2014.07.010>.
- [29] Q. Xu, N.J. Boylan, S. Cai, B. Miao, H. Patel, J. Hanes, Scalable method to produce biodegradable nanoparticles that rapidly penetrate human mucus, *J. Contr. Release* 170 (2013) 279–286, <https://doi.org/10.1016/j.jconrel.2013.05.035>.
- [30] T.G. van Kooten, J.M. Schakenraad, H.C. van der Mei, H.J. Busscher, Influence of substratum wettability on the strength of adhesion of human fibroblasts, *Biomaterials* 13 (1992) 897–904, [https://doi.org/10.1016/0142-9612\(92\)90112-2](https://doi.org/10.1016/0142-9612(92)90112-2).
- [31] C.M. Costello, M.B. Phillipsen, L.M. Hartmanis, M.A. Kwasnica, V. Chen, D. Hackam, M.W. Chang, W.E. Bentley, J.C. March, Microscale Bioreactors for *in situ* characterization of GI epithelial cell physiology, *Sci. Rep.* 7 (2017) 1–10, <https://doi.org/10.1038/s41598-017-12984-2>.
- [32] H.J. Kim, D. Huh, G. Hamilton, D.E. Ingber, Human gut-on-a-chip inhabited by microbial flora that experiences intestinal peristalsis-like motions and flow, *Lab Chip* 12 (2012) 2165–2174, <https://doi.org/10.1039/c2lc40074j>.
- [33] T. Kang, C. Park, J.-S. Choi, J.-H. Cui, B.-J. Lee, Effects of shear stress on the cellular distribution of polystyrene nanoparticles in a biomimetic microfluidic system, *J. Drug Deliv. Sci. Technol.* 31 (2016) 130–136, <https://doi.org/10.1016/J.JDDST.2015.12.001>.
- [34] E. Lee, H.H.G. Song, C.S. Chen, Biomimetic on-a-chip platforms for studying cancer metastasis, *Curr. Opin. Chem. Eng.* 11 (2016) 20–27, <https://doi.org/10.1016/j.coche.2015.12.001>.
- [35] S. Halldorsson, E. Lucumi, R. Gómez-Sjöberg, R.M.T. Fleming, Advantages and challenges of microfluidic cell culture in polydimethylsiloxane devices, *Biosens. Bioelectron.* 63 (2015) 218–231, <https://doi.org/10.1016/j.bios.2014.07.029>.
- [36] F. Yu, W. Hunziker, D. Choudhury, Engineering microfluidic organoid-on-a-chip platforms, *Micromachines* 10 (2019), <https://doi.org/10.3390/mi10030165>.
- [37] D.R. Liston, M. Davis, Clinically Relevant Concentrations of Anticancer Drugs: A Guide for Nonclinical Studies, 2017, <https://doi.org/10.1158/1078-0432.CCR-16-3083>.

- [38] S. Checkley, L. MacCallum, J. Yates, P. Jasper, H. Luo, J. Tolsma, C. Bendtsen, Bridging the Gap between in Vitro and in Vivo: Dose and Schedule Predictions for the ATR Inhibitor AZD6738 OPEN, 2015, <https://doi.org/10.1038/srep13545>.
- [39] D. Anton, H. Burckel, E. Josset, G. Noel, Three-dimensional cell culture: a breakthrough in vivo, *Int. J. Mol. Sci.* 16 (2015) 5517–5527, <https://doi.org/10.3390/ijms16035517>.
- [40] F. Danhier, E. Ansorena, J.M. Silva, R. Coco, A. Le Breton, V. Préat, PLGA-based nanoparticles: an overview of biomedical applications, *J. Contr. Release* 161 (2012) 505–522, <https://doi.org/10.1016/j.jconrel.2012.01.043>.
- [41] M. Boegh, H.M. Nielsen, Mucus as a barrier to drug delivery - understanding and mimicking the barrier properties, *Basic Clin. Pharmacol. Toxicol.* 116 (2015) 179–186, <https://doi.org/10.1111/bcpt.12342>.
- [42] X. Zhang, W. Dong, H. Cheng, M. Zhang, Y. Kou, J. Guan, Q. Liu, M. Gao, X. Wang, S. Mao, Modulating intestinal mucus barrier for nanoparticles penetration by surfactants, *Asian J. Pharm. Sci.* 14 (2019) 543–551, <https://doi.org/10.1016/j.ajps.2018.09.002>.
- [43] S. Varma, J. Voldman, A cell-based sensor of fluid shear stress for microfluidics, *Lab Chip* 15 (2015) 1563–1573, <https://doi.org/10.1039/c4lc01369g>.
- [44] A. Anil, P. Sudheer, Mucoadhesive polymers - a review, *J. Pharm. Res.* 17 (2018) 1–11, <https://doi.org/10.18579/jpcrc/2018/17/1/119566>.
- [45] S. Surassmo, N. Saengkrit, R. Ruktanonchai, K. Suktham, N. Woramongkolchai, T. Wutikhun, S. Puttipipatkachorn, U.R. Ruktanonchai, K. Suktham, N. Woramongkolchai, T. Wutikhun, S. Puttipipatkachorn, Surface modification of PLGA nanoparticles by carbopol to enhance mucoadhesion and cell internalization, *Colloids Surf. B Biointerfaces* 130 (2015) 229–236, <https://doi.org/10.1016/j.colsurfb.2015.04.015>.
- [46] K. Netsomboon, A. Bernkop-Schnürch, Mucoadhesive vs. mucopenetrating particulate drug delivery, *Eur. J. Pharm. Biopharm.* 98 (2016) 76–89, <https://doi.org/10.1016/j.ejpb.2015.11.003>.
- [47] Z. Wu, C. Guo, S. Liang, H. Zhang, L. Wang, H. Sun, B. Yang, A pluronic F127 coating strategy to produce stable up-conversion NaYF<sub>4</sub>:Yb,Er(Tm) nanoparticles in culture media for bioimaging, *J. Mater. Chem.* 22 (2012) 18596–18602, <https://doi.org/10.1039/c2jm33626j>.
- [48] P. Neuzil, S. Giselbrecht, K. Länge, T.J. Huang, A. Manz, Revisiting lab-on-a-chip technology for drug discovery, *Nat. Rev. Drug Discov.* 11 (2012) 620–632, <https://doi.org/10.1038/nrd3799>.
- [49] R. Steele, A. Doiron, R. Shepherd, K. Rinker, Effect of Disturbed Flow on Nanoparticle Uptake in Endothelial Cells, 2011, p. 22.
- [50] E.K. Breitner, S.M. Hussain, K.K. Comfort, The role of biological fluid and dynamic flow in the behavior and cellular interactions of gold nanoparticles, *J. Nanobiotechnol.* 13 (2015) 56, <https://doi.org/10.1186/s12951-015-0117-1>.
- [51] M.L. Graham, M.J. Prescott, The multifactorial role of the 3Rs in shifting the harm-benefit analysis in animal models of disease, *Eur. J. Pharmacol.* 759 (2015) 19–29, <https://doi.org/10.1016/j.ejphar.2015.03.040>.